The popsicle-stick cobra wave

Jean-Philippe Boucher, Christophe Clanet, David Quéré, Frédéric Chevy

The popsicle-stick cobra wave

Jean-Philippe Boucher [1], Christophe Clanet [1], David Quéré [2] and Frédéric Chevy [3]
[1] *LadHyX, UMR 7646 du CNRS, École Polytechnique, 91128 Palaiseau Cedex, France*
[2] *PMMH, UMR 7636 du CNRS, ESPCI, 75005 Paris, France*
[3] *Laboratoire Kastler Brossel, ENS-PSL Research University, CNRS, UPMC, Collège de France, 24, rue Lhomond, 75005 Paris*

The cobra wave is a popular physical phenomenon arising from the explosion of a metastable grillage made of popsicle sticks. The sticks are expelled from the mesh by releasing the elastic energy stored during the weaving of the structure. Here we analyse both experimentally and theoretically the propagation of the wave-front depending on the properties of the sticks and the pattern of the mesh. We show that its velocity and its shape are directly related to the recoil imparted to the structure by the expelled sticks. Finally we show that the cobra wave can only exist for a narrow range of parameters constrained by gravity and rupture of the sticks.

Physics of metastable states is a classical topic of statistical physics [1, 2]. A well known route to relax towards equilibrium is via a nonlinear front which propagates with a constant speed, such as in viral spread [3, 4], bio-chemical reactions [5] or combustion [6, 7]. In mechanics, the domino race provides an example of such a process for a non-connected network [8, 9]. For entangled structures, the question of the optimization of the strength of grillages has been addressed [10, 11] especially because of its role in construction [12] but their stability remains an open question. The same type of question also arises in biological systems, such as in the microtubule catastrophe [13, 14]. Microtubules are assemblies of GDP tubulin arranged in a tubular shape ending with a cap of GTP tubulin. The loss of this cap triggers a rapid depolymerization driven by the release of the stored mechanical strain [15–17]. Here we study a macroscopic version of such a system, namely the so-called "popsicle-stick cobra wave" [18], obtained by releasing a mesh of sticks woven according to Fig. 1.b.

To generate a cobra wave, the whole structure is loaded by the geometrically-constrained bending of the individual sticks and is held together by the red and blue sticks at the end of the mesh (see Fig. 1.b). When one of them is removed, the structure unravels by expelling one

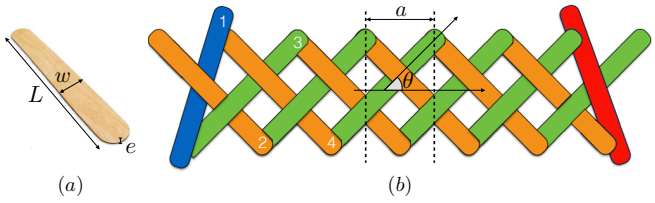

FIG. 1: (a) Picture of a wooden stick with its characteristic parameters : length L, width w, thickness e, mass M, density ρ and Young's modulus E. (b) Schematics of the lattice with definition of the angle θ of the lattice and the period a of the pattern. The blue and red sticks are the sticks that end the lattice. The construction of the lattice starts with the blue stick (number 1), then the sticks are added one after the other (according to the numbering for the first four sticks), with an alternation of orange and green sticks up to the final red stick.

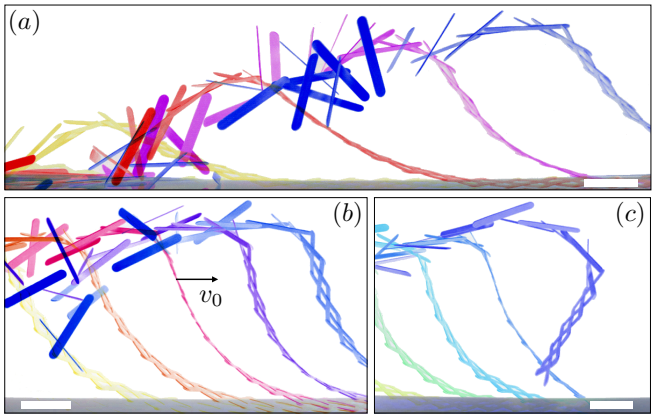

FIG. 2: Time-lapse photographies of the cobra wave obtained with sticks of type-1 (see [19]) for $\theta = 45^o$, from videos taken at 1000 fps with a Photron-Fastcam high-speed camera. The different colors represent the wave at different instants. (a) At the beginning ($\Delta t = 100$ ms between two consecutive images); (b) During the stationary phase ($\Delta t = 70$ ms), with $v_0 \simeq 2.2$ m/s the velocity of the wave front ; (c) At the end ($\Delta t = 70$ ms). Scale bars are 10 cm long.

by one the freed sticks. Due to the asymmetry of the weaving, two very different dynamics occur depending on which stick was initially removed. When the red stick is taken away first, the sticks are expelled upwards and by reaction they pin down the rest of the mesh to the ground (see [19]). The outcome is dramatically different when the blue stick is removed. In this case, the sticks are expelled downwards and they raise the whole structure as presented in Fig. 2.a (see also the movie provided in [19]). After a few hundreds of milliseconds, the shape of the wave reaches a steady state (Fig. 2.b), and propagates at a few meters per second. Both the shape and the velocity remain the same until the wave-front reaches the end of the grillage (Fig. 2.c). In this letter, we combine experimental and theoretical approaches to characterize the velocity and shape of the cobra wave in the steady state.

Since the lifting force raising the lattice originates from the recoil imparted by the expelled sticks, the global dy-

namics of the wave is set by the ejection rate γ and the momentum transferred during the expulsion Mv where M is the mass of a stick and v the velocity of a stick right after expulsion. The time γ^{-1} taken by a stick to exit the mesh is given by L/v, where L is the length of individual sticks (Fig. 1.a). Taking E the Young's modulus, w the width and e the thickness of individual sticks (Fig. 1.a), v can be estimated from the balance between the kinetic energy Mv^2 of a stick after ejection and the bending energy Ewe^5/L^3 stored in each stick blocked by the lattice.

From the previous scaling analysis, we readily deduce the velocity v_0 of the wave-front. Indeed, since the sticks are expelled one by one, we have $v_0 = a\gamma/2$ where a is the spatial period of the pattern (Fig. 1.b). Noting that, up to a geometric factor depending on the angle θ, we have $a \propto L$, both v and v_0 scale as

$$v \simeq v_0 = b(\theta)\sqrt{\frac{E}{\rho}}\left(\frac{e}{L}\right)^2. \qquad (1)$$

where ρ is the mass-density of a stick and $b(\theta)$ is a scaling factor that depends on the geometry of the mesh. With $c = \sqrt{E/\rho}$ the speed of sound in the material, we find that $v_0 \propto c(e/L)^2$. In Fig. 3, we confirm experimentally this scaling for six kinds of wooden sticks (the values of the mechanical and geometric parameters of the different stick models are given in [19]) and we observe that indeed $v \propto v_0$. As expected, the speed does not depend on the width of the sticks and increases quadratically with the ratio e/L. In Fig. 3.i, one can see that the speed of the cobra decreases with the angle of the lattice θ. This trend can be easily understood qualitatively by noting that the velocity of the wave is proportional to the spatial periodicity $a = L\cos\theta/3$.

We now focus on the shape of the wave. The height of the cobra can be understood quantitatively within a generalized version of Euler's elastica theory, where the mesh profile results from a competition between elasticity, gravity and recoil imparted by the expelled sticks [20]. We treat the mesh as a linear continuous medium characterized by a flexion modulus $\bar{K}$ [19] and we describe the expulsion of the sticks by a force $\boldsymbol{F}_0$ and a torque $\boldsymbol{C}_0$ exerted at the free end of the grillage. Describing the shape of the mesh by a profile $\boldsymbol{r}(s,t)$, where s is the curvilinear abscissa (Fig. 4), the local force $\boldsymbol{F}(s,t)$ and torque $\boldsymbol{C}(s,t)$ are given by

$$\boldsymbol{F} = -\bar{K}\partial_s^3\boldsymbol{r} \qquad \boldsymbol{C} = \bar{K}\partial_s\boldsymbol{r}\times\partial_s^2\boldsymbol{r}. \qquad (2)$$

In steady state, the shape of the cobra is constant and moves at the velocity v_0. We therefore have $\boldsymbol{r}(s,t) = \boldsymbol{r}(s' = s - v_0 t)$ and writing Newton's Law for an infinitesimally small element of the mesh leads to the following dynamical equation

$$\mu v_0^2\partial_{s'}^2\boldsymbol{r} = \mu\boldsymbol{g} - \bar{K}\partial_{s'}^4\boldsymbol{r} + \partial_{s'}(T\boldsymbol{\tau}) + \boldsymbol{R}. \qquad (3)$$

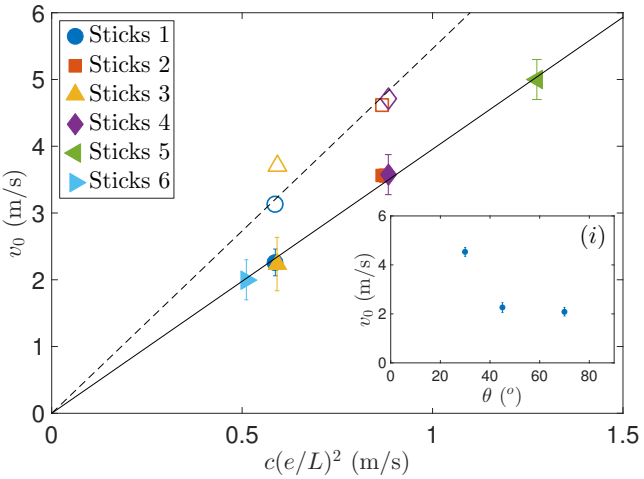

FIG. 3: Speed of the wave-front v_0 (filled dots) and speed of the expelled sticks v (open dots) as a function of a characteristic speed $c(e/L)^2$ for $\theta = 45^o$ and six different kinds of sticks (see [19]). The black line corresponds to the fit $v_0 = 3.95\, c(e/L)^2$ and the dashed line to the fit $v = 5.46\, c(e/L)^2$. (i) Speed of the cobra wave v_0 as a function of the angle of the lattice θ for sticks of type-1.

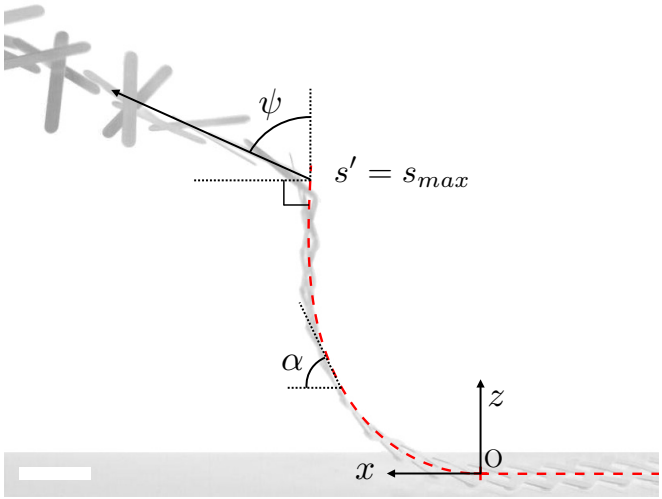

FIG. 4: Experimental cobra profile for sticks of type-4. The steady profile (red dashed line) is described theoretically by a parametric curve $\boldsymbol{r}(s')$ where s' is the linear abscissa. α is the angle between the mesh and the horizontal axis and ψ the angle between the velocity of the expelled sticks and the tangent vector in $s' = s_{max}$. The scale bar is 10 cm long.

where $\mu = 2M/a$ is the linear mass density of the cobra, T the longitudinal tension, $\boldsymbol{\tau}$ the tangent unit vector and $\boldsymbol{R}$ the ground reaction. We assume that the contact with the ground occurs for $s' \leq 0$, so that $z(s' \leq 0) = 0$ and $\boldsymbol{R}(s' \geq 0) = 0$, and $s_{\max}$ is the total mesh-length rising above the ground. Projecting Eq. (3) on the tangent and normal directions, these equations can be recast into a closed equation for the curvature $\Gamma = |\partial_s^2\boldsymbol{r}|$

$$\frac{1}{2}\left[\frac{d^3\Gamma^2}{d\alpha^3}+\frac{d\Gamma^2}{d\alpha}\right]=\frac{\mu g}{\bar{K}}\left[\frac{2\sin\alpha}{\Gamma}+\frac{\cos\alpha}{\Gamma^2}\frac{d\Gamma}{d\alpha}\right]. \quad (4)$$

where α is the local angle between the mesh and the horizontal axis.

This equation is of third order in α and thus requires three boundary conditions to be solved. We obtain these conditions by writing the stress at the free end $\alpha_{\max} = \alpha(s_{\max})$ of the mesh, namely:

$$C_0 = \bar{K}\Gamma \quad (5)$$
$$F_{\parallel} = T + \bar{K}\Gamma^2 \quad (6)$$
$$F_{\perp} = -\frac{K}{2}\frac{d\Gamma^2}{d\alpha} \quad (7)$$

where $F_{\parallel} = \boldsymbol{F}_0 \cdot \boldsymbol{\tau}$ and $F_{\perp} = \boldsymbol{F}_0 \cdot \boldsymbol{n}$ and the right-hand side terms are taken at $\alpha = \alpha_{\max}$. A fourth condition is required by the fact that, contrary to the elastica problem where the length of the beam is fixed, we must here determine self-consistently the mesh length rising above the ground. To close the system, we therefore impose the usual mobile contact-point condition $\Gamma(\alpha = 0) = 0$ that assumes that there is no adhesion energy between the mesh and the ground [21].

On the one hand, the forces can be calculated from the momentum transfer between the lattice and the expelled sticks and we have $F_{\perp} = \mu v_0 v \sin\psi$ and $F_{\parallel} = \mu v_0(v_0 - v\cos\psi)$.

On the other hand, the torque exerted at the free end of the cobra can be neglected. Indeed, assuming that all the elastic energy is converted into rotational energy of the sticks, we have the upper bound $C_{\max} = \gamma\sqrt{2IE_{\rm el}}$ where I is the moment of inertia of a stick. In Eq. (5) and (6), the force must be compared to $C^2/\bar{K}$. We have

$$\frac{C^2}{\bar{K}F} \simeq \frac{\gamma^2 I(Ke^2/L^3))}{K\gamma M v_0} \simeq \left(\frac{e}{L}\right)^2 \ll 1,$$

where $K \simeq \bar{K}$ is the flexion modulus of a single stick [19] and we have used the fact that $v \simeq v_0 \simeq \gamma L$ and $I \simeq ML^2$. We thus see that for thin sticks, the torque does not affect much the shape of the cobra.

Eq. (4) can be solved numerically in the general case using the shooting method and the height of the cobra can be obtained from

$$H = \int_0^{\alpha_{\max}} \frac{\sin\alpha}{\Gamma(\alpha)} d\alpha. \quad (8)$$

The analysis of equations (4-8) shows that H follows the general scaling

$$H = \sqrt{\frac{\bar{K}}{\mu v_0 v}}\, h_\psi\left(\Lambda = g\sqrt{\frac{\bar{K}}{\mu v_0^3 v^3}}\right). \quad (9)$$

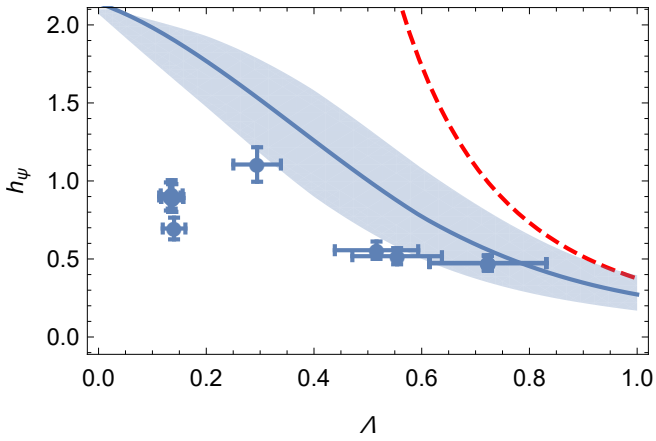

FIG. 5: Dimensionless height h_ψ as a function of the dimensionless number $\Lambda = g\sqrt{\bar{K}/(\mu v_0^3 v^3)}$ which compares gravity and elasticity, for the six different kinds of sticks ([19]). The solid line corresponds to the prediction of Eq. (4-8) for $\psi = 60^o$. The shaded band corresponds to the observed 10^o variations of the ejection angle. The red dashed line represents the large Λ expansion $h_\psi \simeq 2\sin^4\psi/3\Lambda^3$ for $\psi = 60^o$.

When gravity can be neglected, Eq. (4) can be solved analytically and yields $\Gamma = \Gamma_0\sqrt{\cos(\psi-\alpha)-\cos(\psi)}$ with $\Gamma_0 = \sqrt{2\mu v v_0/\bar{K}}$. We then obtain $\alpha_{\max} = 2\psi$ and the dimensionless height can be expressed in terms of the elliptic integrals $\mathcal{E}$ and $\mathcal{K}$ [22] with

$$h_\psi(0) = 2\sin(\psi)\left[2\mathcal{E}(\sin(\psi/2)) - \mathcal{K}(\sin(\psi/2))\right]. \quad (10)$$

For large values of Λ, gravity becomes dominant and the cobra does not rise as high. In this regime, $\alpha_{\max} \to 0$ and we can therefore neglect the lower order derivatives in each sides of Eq. (4) leading to the simplified expression

$$\frac{d^3\Gamma^2}{d\alpha^3} = \frac{2\mu g}{\bar{K}\Gamma^2}\frac{d\Gamma}{d\alpha}. \quad (11)$$

This equation can be solved analytically leading to an asymptotic behaviour $h_\psi \simeq 2\sin^4\psi/3\Lambda^3$.

The asymptotic behaviours obtained in both the weak and strong gravity regimes can be understood by a straightforward argument. We note first that Eq. (7) and (8) lead to the following scalings

$$F_{\perp} \simeq \bar{K}\frac{\Gamma_0^2}{\alpha_{\max}} \qquad H \simeq \frac{\alpha_{\max}^2}{\Gamma_0}. \quad (12)$$

We can then distinguish two regimes. For small g, the height is saturated and $\alpha_{\max} \simeq 1$, hence $\Gamma_0 \simeq \sqrt{F_\perp/\bar{K}}$ and $H \simeq \Gamma_0^{-1} \simeq \sqrt{\bar{K}/F_\perp}$. The scaling for H yields the condition $h_\psi \simeq 1$ for weak gravity. Using Eq. (1), we can express v_0 and $F_\perp$ with K, e and L. We then obtain a simple scaling for $H \simeq L^2/e$, which does not

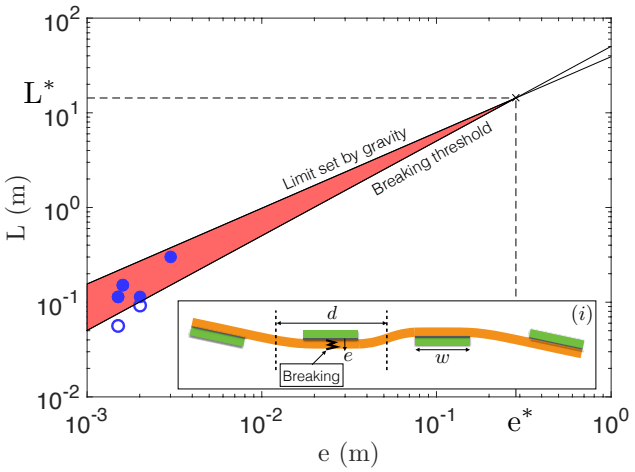

FIG. 6: Set of parameters (e, L) for which a cobrastick wave can be observed (red region). This region is delimited by the two conditions given in Eq. (14) and (16) : the limit set by gravity $L_{\max} = \left(36Ee^4/\rho g\right)^{1/5}$ and the breaking limit $L_{\min} = 1.5 \times 3\sqrt{E/\sigma^* e}$. Filled blue dots : sets of parameters for which the cobrastick wave is observed. Open blue dots : sets of parameters for which the cobrastick wave could not be observed (the sticks are too small and therefore break). (i) Schematics of the shape of a stick in the lattice with the most probable breaking region.

depend any more on the elasticity of the mesh. This purely geometric scaling stems from the fact that, when gravity is negligible, stick elasticity provides both the thrusting and restoring forces responsible for the shape of the mesh.

For heavy sticks, the lattice is almost horizontal and the value of $\alpha_{\max}$ is set by the balance between $F_\perp$ and the weight. The length of the cobra being $s_{\max} \simeq \alpha_{\max}/\Gamma_0$, we have thus the additional condition

$$F_\perp \simeq \frac{\mu g \alpha_{\max}}{\Gamma_0}. \tag{13}$$

Combining Eq. (12) and (13) yields the condition $\alpha_{\max} \simeq \Lambda^{-2}$ and $h_\psi \simeq 1/\Lambda^3$. The transition between the two regimes occurs for $\Lambda \simeq 1$.

We now compare the previous model to our measurements. We measured the velocity v and the angle ψ at which the sticks are expelled. We observe that for almost all stick models, ψ varies between 50^o and 70^o. In Fig. 5, we compare our measurements to the predicted value $h_{\psi=60^o}$ without any adjustable parameter. Except in the weak-gravity regime, we observe a relatively good agreement between experiment and theory. We attribute the saturation of the height of the cobra-wave for small Λ to the strong curvature of the mesh (in this regime the radius of curvature is only a few times larger than stick length), leading to a breakdown of the underlying assumptions of the theoretical model. For instance the validity of the continuum approximation for the description of the mesh, or the linear approximation for the bending energy. Friction can also play a larger role, and the strong deformation can weaken the structure, preventing it from reaching its predicted height.

Finally, we discuss the condition of existence of the cobra-wave. The first requirement is that the curvature energy stored in a single stick ($E_{el} = 18Ewe^5/L^3$) should overcome the gravitational energy ($E_g = \rho g w e L^2/2$). This leads to an upper bound for the length L of the sticks:

$$L < L_{\max} = \left(\frac{36Ee^4}{\rho g}\right)^{1/5}. \tag{14}$$

However, the length L of the sticks cannot be too small because if so it becomes impossible to build the lattice: the sticks either break or slide over each other destroying the lattice. The breaking condition is derived from a simple scaling law for the bending stress in a beam which sets an upper limit for the curvature of a stick in the lattice (Fig. 6.i) :

$$\mathcal{C} \sim \frac{e}{d^2} < \frac{\sigma^*}{Ee}, \tag{15}$$

where the length $d = (L-w)/3$ is defined in Fig. 6.i and σ^* is the bending stress at rupture of the material. We then get a lower bound for the length L of the sticks

$$L > L_{\min_b} \sim 3\sqrt{\frac{E}{\sigma^*}}e + w. \tag{16}$$

For wooden sticks, these two conditions set the boundaries of the cobra-wave region of existence. The phase diagram (e, L) is plotted in Fig. 6 with the region of existence of the cobrastick wave in red, assuming the width w to be negligible compared to the length L of the sticks. In particular, this region is semi-infinite, the maximal length being $L^* \sim 10$ m which corresponds to a maximal thickness $e^* \sim 25$ cm.
We identify a third condition on L which is related to the friction of the sticks and can be obtained from Coulomb's law of friction

$$L > L_{\min_f} \sim \frac{3e}{f} + 4w, \tag{17}$$

where f is the coefficient of static friction.

It is noticeable that the relative position of the breaking threshold and the friction threshold depends on the material of the sticks. For instance, for sticks made of PVC, unlike wooden sticks, the friction threshold is higher than the breaking threshold and is therefore the one that sets the lower bound for the length of the sticks.

In conclusion, we have shown that the shape of the popsicle-stick cobra wave was the result of a competition between on the one hand elastic and gravitational restoring forces and on the other hand the thrust provided by the expulsion of the sticks. Depending on the relative importance of gravity, we identified two asymptotic regimes. In particular, for negligible gravity, the

cobra rises at a height which is solely set by the weaving pattern and the dimensions of single sticks. Finally, we showed that the Cobra wave can only exist in a narrow region of the parameter space bounded by gravity and rupture of the sticks. In future work, we will study more carefully the local expulsion dynamics of individual sticks to clarify the role of the weaving pattern.

Acknowledgments

This work was inspired by one the problems of the 2016 edition of the International Physicists' Tournament (IPT). The authors acknowledge fruitful discussions with Basile Audoly, Daniel Suchet and the ENS and École Polytechnique IPT teams.

[1] L.D. Landau and E.M. Lifshitz. *Statistical Physics*, volume 5. Pergamon Press, 1980.
[2] J.S. Langer. Statistical theory of decay of metastable states. *Annals of Physics*, 54:258–275, 1969.
[3] R.A. Fisher. The wave of advance of advantageous genes. *annals of eugenics*, 7(4):353–369, 1937.
[4] A. Kolmogorov, I. Petrovsy, , and N. Piskounov. Study of the diffusion equation with growth of the quantity of matter and its applications to a biological problem. *Moscow University Mathematics Bulletin*, page 105, 1989.
[5] J.D. Murray. *Mathematical Biology*. Springer, 2000.
[6] Ya. B. Zeldovich, G.I. Barenblatt, V.B. Librovich, and G.M. Makhviladze. *The mathematical theory of combustion and explosions*. Consultants Bureau, 1985.
[7] P. Clavin and G. Searby. *Combustion waves and fronts in flows*. Cambridge University Press, 2016.
[8] W.J. Stronge. The domino effect: a wave of destabilizing collisions in a periodic array. *Proc. Roy. Soc. London A*, 409:199–208, 1987.
[9] W.J. Stronge and D. Shu. The domino effect: successive destabilization by cooperative neighbours. *Proc. Roy. Soc. London A*, 418:155–163, 1988.
[10] G. I. N. Rozvany. Grillages of maximum strength and maximum stiffness. *Int. J. mech. Sci.*, 14:651–666, 1972.
[11] T. Tarnai. Duality between plane trusses and grillages. *Inl. J. Solids Slructures*, 25:1395–1409, 1989.
[12] P.M. Stylianidis, D.A. Nethercot, B.A. Izzuddin, and A.Y. Elghazouli. Robustness assessment of frame structures using simplified beam and grillage models. *Engineering Structures*, 115:78–95, 2016.
[13] I. M. Cheeseman and A. Desai. Molecular architecture of the kinetochore–microtubule interface. *Nature Review, Molecular Cell Biology*, 9:33–46, 2008.
[14] A. Desai and T. Mitchison. Microtubule polymerization dynamics. *Annu. Rev. Cell Dev. Biol.*, 13:83–117, 1997.
[15] T.Mitchison and M. Kirschner. Dynamic instability of microtubule growth. *Nature*, 312(15):237–242, 1984.
[16] T.Mitchison and M. Kirschner. Microtubule assembly nucleated by isolated centrosomes. *Nature*, 312(15):232–237, 1984.
[17] H. Bowne-Anderson, A. Hibbel, and J. Howard. Regulation of microtubule, growth and catastrophe: Unifying theory and experiment. *Trends in Cell Biology*, 25(12):769–779, 2015.
[18] `https://en.wikipedia.org/wiki/Stick_bomb`. Accessed: 2016-12-13.
[19] Supplementary materials.
[20] Basile Audoly and Yves Pomeau. *Elasticity and geometry: from hair curls to the non-linear response of shells*. Oxford University Press, 2010.
[21] R Burridge and JB Keller. Peeling, slipping and crackingsome one-dimensional free-boundary problems in mechanics. *SIAM Review*, 20(1):31–61, 1978.
[22] Milton Abramowitz and Irene A Stegun. *Handbook of mathematical functions: with formulas, graphs, and mathematical tables*. Courier Corporation, 1964.

Supplementary materials

I. CHARACTERISTICS OF THE STICKS

We measured the Young modulus E of our sticks through measurements of the load on a force sensor for given deflections of the sticks and we found $E \simeq 15\,\mathrm{GPa}$. We estimated the bending stress at rupture of the sticks $\sigma^* \simeq 120\,\mathrm{MPa}$ experimentally through a three-point flexural test.

Sticks	L (mm)	w (mm)	e (mm)	M (g)
1	150	18.0	1.6	2.64
2	114	14.3	1.5	1.45
3	150	9.0	1.6	1.30
4	114	7.0	1.5	0.70
5	113	9.0	2.0	1.23
6	150	17.0	1.5	2.45
7	56	7.0	1.5	0.25
8	93	9.0	2.0	1.02

TABLE I: Geometrical and mechanical properties of the wooden sticks used in this study. Sticks 7 and 8 are sticks for which the cobrastick wave was not observed and appear in Fig. 6.

II. ELASTIC MODULUS OF THE MESH

The elastic properties of the mesh are described by a bending energy

$$E_{\mathrm{el}} = \frac{\bar{K}}{2} \int \Gamma(s)^2 \, \mathrm{ds}, \tag{18}$$

where Γ is the local curvature of the mesh and $\bar{K}$ the effective bending modulus. $\bar{K}$ is determined experimentally by measuring the load on a force sensor for given deflections of the mesh. In Fig. 7, we plot the measured value $\bar{K}$ normalized by the bending modulus of a single stick $K = EI_\perp$ (where $I_\perp = we^3/12$ is the second moment of area) as a function of the weaving angle θ. For $\theta = \pi/4$, we find in particular $\bar{K} \simeq 0.7K$. Assuming that the sticks are simply wrapped with an angle θ on a cylinder of radius Γ^{-1}, one obtains $\bar{K} = 3K\cos(\theta)^3$. This scaling is close to the fitted behaviour $\bar{K}/K = k_0\cos(\theta)^3$, with $k_0 = 2.2$. The discrepancy with the expected value $k_0 = 3$ may come from the torsion of the sticks in the mesh or from the fact that even in the absence of macroscopic bending of the mesh, individual sticks are already bent by the weaving of the mesh.

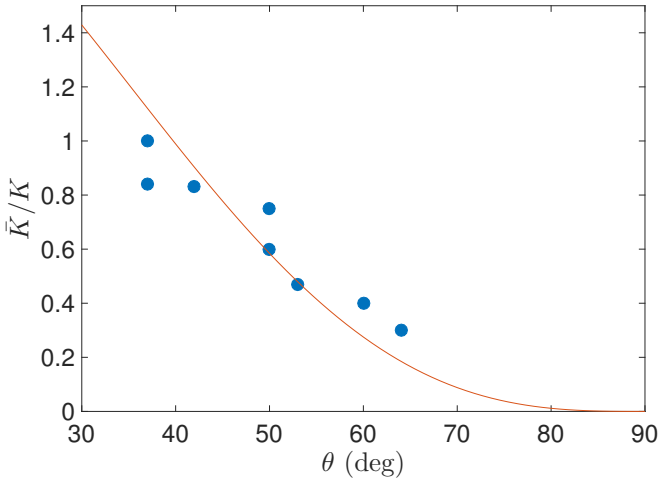

FIG. 7: Normalized bending modulus of the mesh $\bar{K}/K$ as a function of the weaving angle θ obtained experimentally by measuring the force on a load cell for imposed deflections of the mesh. Solid line: fit of the data using the theoretical function $\bar{K}/K = k_0 \cos(\theta)^3$ with $k_0 = 2.2$, close to the expected value $k_0 = 3$ derived from a purely geometric argument.